Envisat ASAR polarization experiment in Peter the Great Bay, Japan Sea: Preliminary results

Leonid M. Mitnik, Vyacheslav A. Dubina & Oleg G. Konstantinov
Department of Satellite Oceanography, V.I. Il'ichev Pacific Oceanological Institute, FEB RAS, Vladivostok, Russia, e-mail: mitnik@poi.dvo.ru

Keywords: Envisat ASAR, polarization features, slicks, sea surface roughness, internal waves

ABSTRACT: A series of the ASAR images with Alternating Polarization (AP) was acquired over Peter the Great Bay, Japan Sea in 2003-2005. Only Horizontal-Horizontal (HH) and Vertical-Vertical (VV) polarization combination was used with two different mean incidence angle θ: 18.3° and 22.5°. Additionally, the same scenes were sensed on 23 September 2004 by ERS-2 SAR with a time delay about 30 min after ASAR acquisition. The main aim was to study the polarimetric signatures of the sea surface caused by the oceanic dynamic phenomena as well as by natural and anthropogenic slicks for later use for their detection and classification. During ASAR and SAR data acquisition, ground-truth measurements of sea surface temperature, wind speed and direction as well as polarization images of the sea surface recorded by a polarization videosystem were arranged at POI Marine stations and at several coastal stations. Wind fields were also retrieved from SAR images using CMOD-4 scatterometer algorithm. The wind speed during satellite observations did not exceed 7 m/s and as a result the radar signatures of slicks, eddies, currents, and internal waves were revealed on the SAR images. The HH and VV radar cross-sections σ_o^{HH} and σ_o^{vv} computed from ASAR data decreased with θ and the polarization ratio $P = \sigma_o^{VV} / \sigma_o^{HH}$ increased. Variations of P in the areas around the slicks reached 2-4 dB that calls for further investigations.

1 INTRODUCTION

Among the new specificities of the Envisat ASAR, polarization diversity makes the instrument very promising. The Alternating Polarization (AP) mode provides two simultaneous images from the same area with three possible polarization combinations: HH and VV, HH and HV, VV and VH with high spatial resolution as in single polarization mode but with degraded radiometric resolution. There is considerable interest in the AP Mode for oceanic dynamic phenomena detection against the variable background. From current research results using airborne real aperture radar or synthetic aperture radar data, it follows that a combination of VV and HH polarizations allows to discriminate the surface imprints of atmospheric and oceanic phenomena. Experimental results indicate that oceanic features such as internal waves, fronts and sea floor topography tend to appear somewhat better with HH than with VV polarization. In contrast, sea surface imprints of atmospheric features (convective cells and rolls, etc.) appear to be more visible with VV polarization than with HH polarization. Films of surfactants both natural (mainly biogenic) and man-made (oil spills) have manifested themselves on satellite SAR images in a form of dark bands and patches at any polarization when the wind speed is W < 6-7 m/s. These films can serve as indicator of oceanic dynamic processes like fronts, currents, eddies, upwellings, internal waves, etc. both at VV and HH polarization. In connection with this an advantage of alternating polarizations, VV and HH data over one

polarization, VV or HH data in phenomena/background discrimination should be studied in a wide range of sensing geometry and environmental parameters variations however at W < 6-7 m/s.

2 DATA

Envisat ASAR and ERS-2 SAR sensing of Peter the Great Bay, Japan Sea was carried out in different seasons. The boundaries of SAR frames and the location of POI Marine stations and Far Eastern Marine Reserve are sketched in Figure 1a. The area of Cape Shults Marine station where measurements of the sea surface roughness with polarization spectrophotometer were performed and artificial slicks were created from a yacht is depicted in Figure 1b.

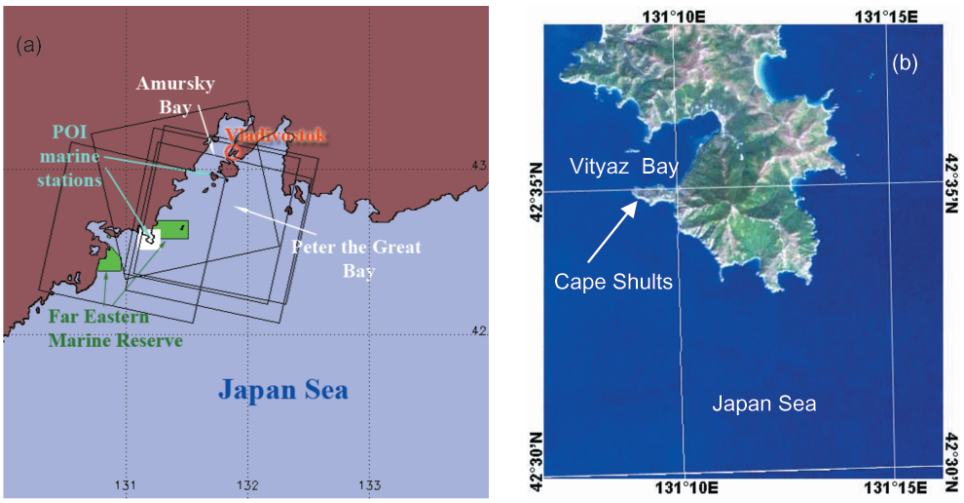

Figure 1. Scheme of Peter the Great Bay with the boundaries of Envisat ASAR and ERS-2 SAR images used in the study. Arrows indicate the location of POI Marine stations and Far Eastern Marine Reserve (a). Cape Shults Marine Station, Vityaz' Bay and the open regions of the Japan Sea where in situ data were collected and experiments with artificial slicks were conducted (b).

Satellite title, date and time of acquisition, wind speed and direction, air sea difference ΔTas = Ta–Ts, where Ta is the air temperature near the sea surface, Ts is the sea surface temperature, as well as the incidence angle θ of Cape Shults area and the values of the Normalized Radar Cross Section (NRCS) at V- and H-polarizations σ_o^{VV} and σ_o^{HH} to the south of Cape are given in Table 1.

Table 1. Envisat ASAR VV- and HH-pol images acquired over Peter the Great Bay.

SAR product	Date	Time (UTC)	Wind speed W (m/s)	Wind direction (deg)	θ (deg)	ΔTas (°C)	σ_o^{VV} (dB)	σ_o^{HH} (dB)
ASAR AP	20 Sep 2003	01:33			21.7		–5.8	–6.4
ASAR AP	6 May 2004	01:36	6.0–7.0	180*	17.5		–0.5	–2.0
ASAR AP	12 July 2004	01:30	3.5–4.0	135	25.8	0.3	–10.3	–13.1
ASAR AP	15 July 2004	01:36	3.0–3.5	225*	17.5		–6.6	–8.8
ASAR AP	20 Sep 2004	01:30	3.0–4.0	320	25.8	–2.9	–12.4	–14.9
SAR PRI	20 Sep 2004	01:59	3.0	300	26.0	–2.1	–6.3	
ASAR AP	23 Sep 2004	01:36	2.0–3.0	315*	17.5	–2.9	–4.0	–5.3
ASAR AP	23 Sep 2004	12:54	4.0 ?	180	15.9		–1.1	–1.9
ASAR AP	10 Feb 2005	12:54		315	15.9			

*Winds were measured at the Pelis Island located at the north-east of Cape Shults.

Ground truth measurements were carried out at Cape Shults and Popov Island as well as at several coastal and island points before, during and after ENVISAT and ERS-2 overpasses. They included the sea surface temperature, wind speed and direction, air temperature and humidity. The acquisition of meteorological characteristics and water temperature at Cape Shults was carried out from a pier, a coastal vantage point and from a yacht. Sea surface roughness characteristics were measured with a system of light floats and with single float and calibration spheres as well as with a developed polarization spectrophotometer [1] at Cape Shults station only. On 12 and 15 July artificial slicks were produced with oleic acid (OLE) in the Vityaz' Bay and in the open sea in the south of Cape Shults (Figure 1b). Spreading and detectability of artificial slicks were studied using video and digital cameras and special calibration floats. Ancillary satellite images (NOAA AVHRR, Terra and Aqua MODIS and Aqua AMSR-E), QuikSCAT SeaWinds-retrieved wind fields were collected for interpretation of radar signatures and development of multi-sensor algorithms.

3 DATA PROCESSING

The NRCS values were computed for the square areas of the size of 100 m × 100 m for each ASAR/SAR image using BEST tool (http://envisat.esa.int/services/best/). The values σ_o^{HH} and σ_o^{VV} given in Table 1 were found for the areas with the uniform brightness distribution near Cape Shults in the size of 1 km × 1 km.

CMOD4, the most commonly used scatterometer algorithm, described by a function [2]:

$$\sigma_o^{VV} = a(\theta)W^{\gamma(\theta)}[1 + b(\theta)\cos\phi + c(\theta)\cos 2\phi) \quad (1)$$

where θ is the local incident angle, $y(\theta)$ is the power law dependence on wind speed, and ϕ is the angle between the radar look direction and the wind direction was used for wind speed retrieval when information on wind direction was available. (Usually assumed that the wind speed W is measured at 10 m above the surface with neutral atmospheric stability).

Wind fields were also retrieved from the measured σ_o^{HH} values using a polarization ratio equation suggested by Thompson et al. [3] and Thompson and Beal [4]

$$\sigma_o^{HH}/\sigma_o^{VV} = (1 + \alpha\tan^2\theta)/(1 + 2\tan^2\theta) \quad (2)$$

and CMOD4 scatterometer algorithm. Calculations were carried out at variations of parameter α to select its value providing better correspondence of wind fields retrieved from σ_o^{VV} and from σ_o^{HH} values.

A polarization ratio $P = \sigma_o^{VV}/\sigma_o^{HH}$ was computed to reveal its changes caused by modulation of the sea surface roughness by oceanic dynamic phenomena at different incidence angles.

4 RESULTS

Envisat ASAR image with VV-polarization acquired from a descending orbit 12367 on 12 July 2004 is shown in Figure 2a. The image covers 100 × 100 km^2 centred around 42°40′N, 131°50′E. The incidence angle varied between 18.7 and 26.2 degrees over the image. Wind field was retrieved from σ_o^{VV} values using scatterometer algorithm (1). The W values vary from 2 till 7 m/s (Figure 2b). Wind speed measurements at several coastal points in Peter the Great Bay and on yacht in Vityaz' Bay and at the south of Cape Shultz (Figure 1) confirm satellite estimates.

H-polarization winds were generally larger than those from V-pol at all values of parameter α. ($\alpha = 0$ corresponds to the polarization ratio predicted by Bragg scattering and $\alpha = 2$ corresponds to CMOD4). The average difference reached 3.7 m/s at $\alpha = 0.6$ (determined from RADARSAT data) and decreased to 1.67 m/s at $\alpha = 2$.

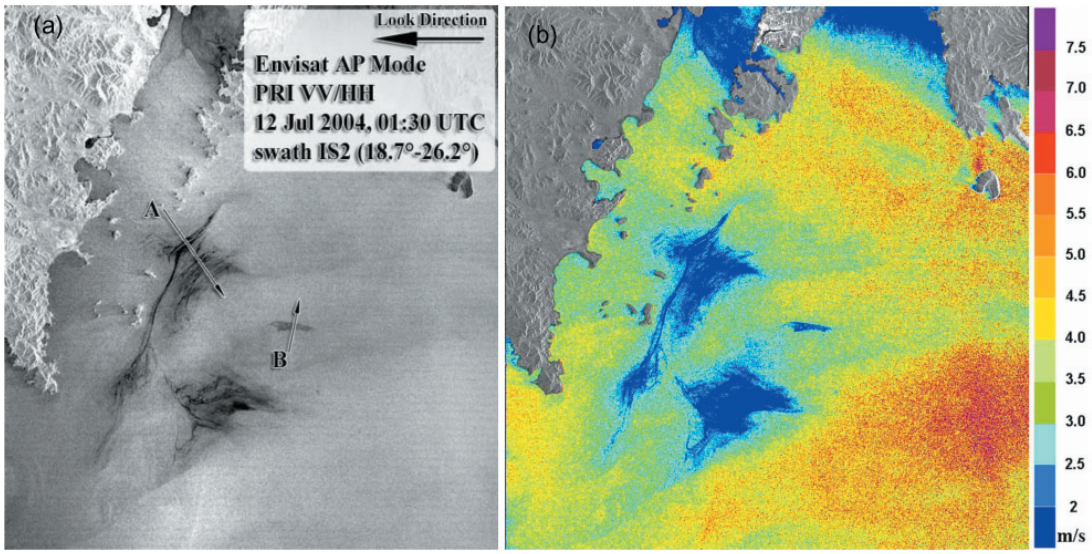

Figure 2. Envisat ASAR image of Peter the Great Bay acquired on 12 July 2004 at 01:30 UTC with vertical polarization (a) and surface wind field derived from the Normalized Radar Cross Section values with scatterometer function (1) (b). Biogenic slicks and oil spills damp the small-scale roughness and the wind retrieval becomes impossible. The slick-covered areas (at the bottom left) as well as the areas with $W \leq 2$ m/s have a dark tone in Figure 2a and a blue tone in Figure 2b.

There are several slick bands and patches on the image which are distinguished from the surrounding waters by a dark tone. The variations of the NRCS with VV- and HH-polarizations along section A crossing the biogenic slicks and section B crossing an oil slick are given in Figure 3a,b. The profiles were computed by averaging of 11 pixels with a size of 25 m × 25 m and application of moving average along section with window width of 7 pixels. The damping degree (contrast) reached 10-15 dB for biogenic slicks both on VV and on HH polarizations. The contrast of oil slick against the surrounding waters was only 3-4 dB very likely due to 'age' of the slick.

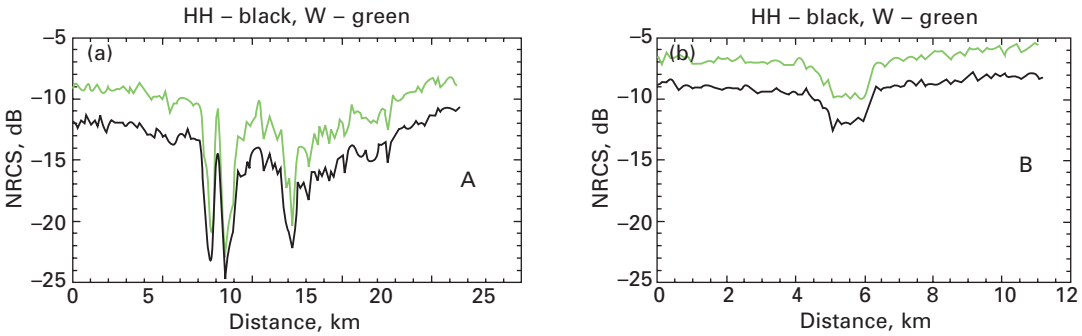

Figure 3. Profiles of Normalized Radar Cross Section (NRCS) across biogenic slicks (a) and oil spill (b) at vertical (green lines) and horizontal (dark lines) polarizations along sections A and B shown in Figure 2a.

Consider the variations of polarization ratio $P = \sigma_o^{VV} / \sigma_o^{HH}$ in the area covered by biogenic slicks depicted on a fragment of the ASAR image with a size of 20 km × 20 km (Figure 4a). Average incidence angle for the fragment is 22°. The wind speed around the slick area varied from 2.5 to 4 m/s (Figure 2b). At first the NRCS values at VV- and HH-polarization were computed for the whole image for pixel size of 25 m × 25 m. Then the NRCS profiles were found for three sections A, B and C each of which represented a band of the width of 21 pixels. The location of sections and their directions are marked by arrows in Figure 4a. The direction of the sections was mainly normal to slick bands. At last a polarization ratio profile for each section was calculated as

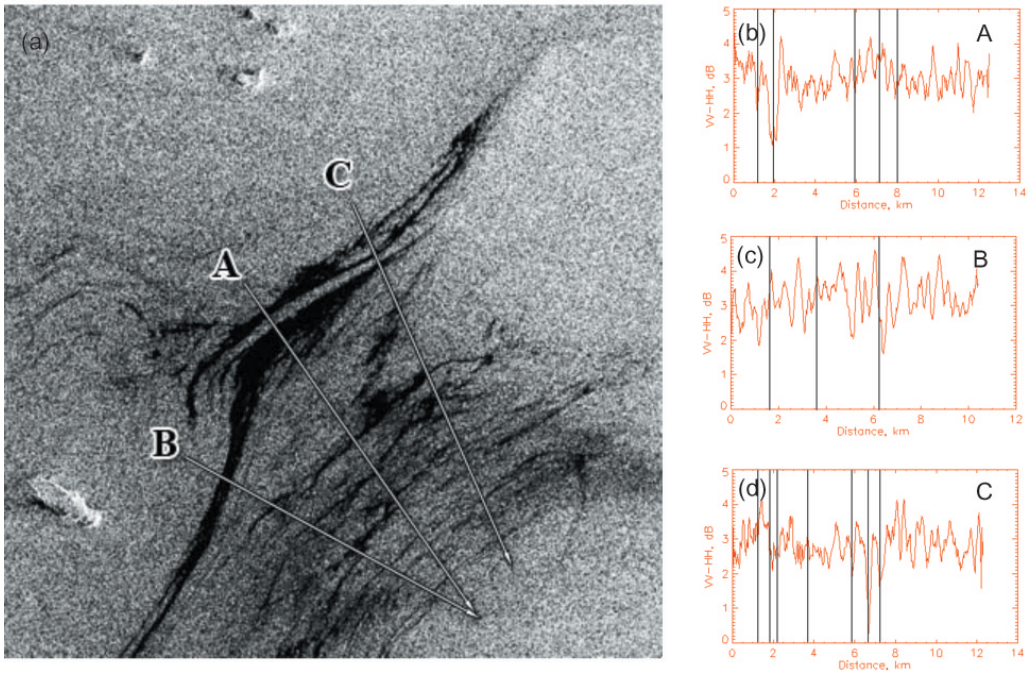

Figure 4. A fragment of Envisat ASAR image for 12 July 2004 with plentiful filamentary slicks (a). Arrows indicate direction of sections A, B and C for which polarization ratio profiles (b), (c) and (d) were computed.

a ratio of the average NRCS values at VV and HH-polarizations with subsequent moving average along the section with a window width of 7 pixels. The P-profiles are given in Figures 4b,c,d. Dark vertical lines mark the location of the individual narrow or wide slick bands.

Polarization ratio along profiles is characterized by large variability. The largest changes are typically (but not always!) observed near the slick bands. Polarization ratio variations should be studied in the broader range of environmental parameter variability, at higher spatial resolution and at larger incidence angles.

The polarization ratio as a function of the incidence angle was computed from ASAR data obtained on 12 and 15 July 2004 at W = 3-5 m/s (about 60000 points). Each point in Figure 5 defines P value for an area of the size of 100 m × 100 m. The average P-values increase from about 1.5 dB at θ = 14.5-15° to 2.8 at θ = 25.5-26°. The increase of P with incidence angle confirms data by Mouchel et al. [5]. Deviations from the average values (white line in Figure 5) are important: rms is 1.14 dB at θ = 19-21° and 1.03 dB at θ = 24-26°.

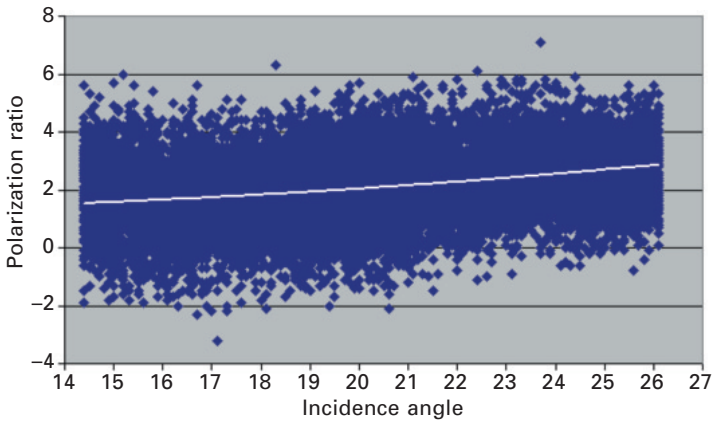

Figure 5. Dependence of polarization ratio on incidence angle.

Roughness parameters were retrieved from displacements of light floats on the sea surface. The displacements were determined by processing of series of images recorded by an optical video system during Envisat ASAR image acquisition [1].

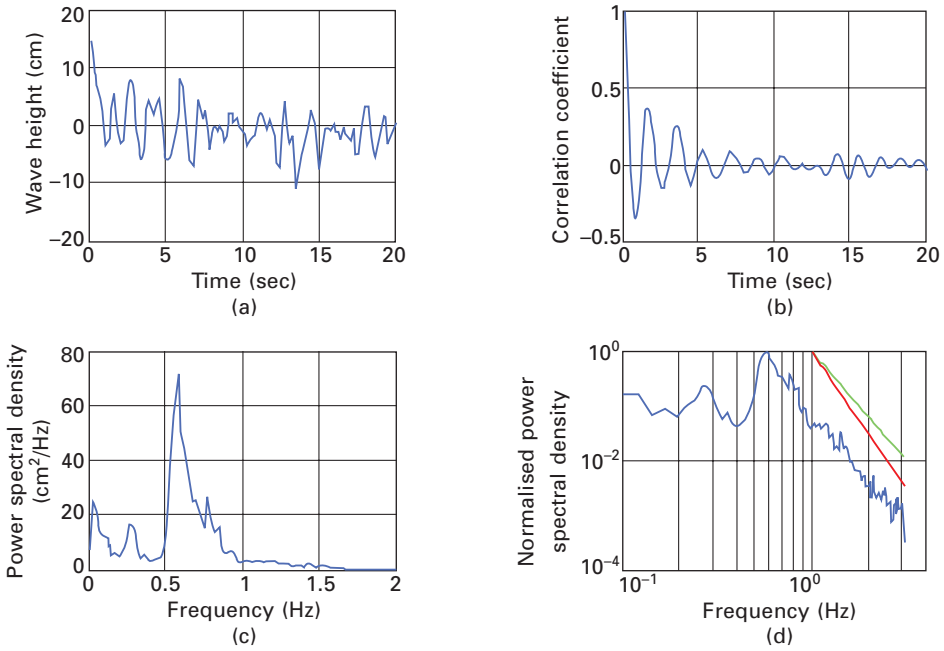

Figure 6. Retrieved wave height (a), correlation function (b), power spectral density (c) and normalized power spectral density (d) computed for realization consisting of 2000 points. Slope of green line $\alpha = -4$ and slope of red line $\alpha = -5$. Measurements were conducted on 12 July 2004 at 1:30 UTC during Envisat ASAR sensing.

5 INDICATION OF OCEANIC DYNAMIC PHENOMENA

Surface manifestations of internal waves were often on ERS-1/2 SAR and Envisat ASAR images covering both the coastal zone and the open Japan Sea [6]. Their parameters estimated by processing data obtained by coastal mooring stations as well as by satellite sensors varied in a wide range. Figure 7 shows Envisat ASAR image acquired on 23 September 2004 at 01:36 UTC. A narrow dark band – very likely a local atmospheric front – crosses the image almost in a diagonal. Surface imprints of oceanic internal waves moving on shore are distinguished in the south-eastern part of the image. Front parts of the individual waves are brighter than the background as opposite to their rear parts which are darker than the background. The intensity of internal waves is high enough: they produce clear imprints in the dark areas where small-scale surface waves are absent. The NRCS profiles at VV- and HH-polarizations as well as polarization ratio profiles were computed for sections A and B. They are presented in Figures 7b-e. Internal waves in the area under study were also detected on Terra and Aqua MODIS 250-m resolution images acquired on 22 September. Riverine waters are often form fronts and biogenic slicks on the sea surface. Elongated slick originating from a river in Vityaz' Bay was recorded by a coastal video system [1]. The same slick was clearly identified on Envisat ASAR VV- and HH-polarization images (Figure 8).

6 CONCLUSIONS

A series of the ASAR images with VV- and HH-polarization was acquired over Peter the Great Bay, Japan Sea both in warm and cold seasons in 2003-2005. Ground truth data including the measurements

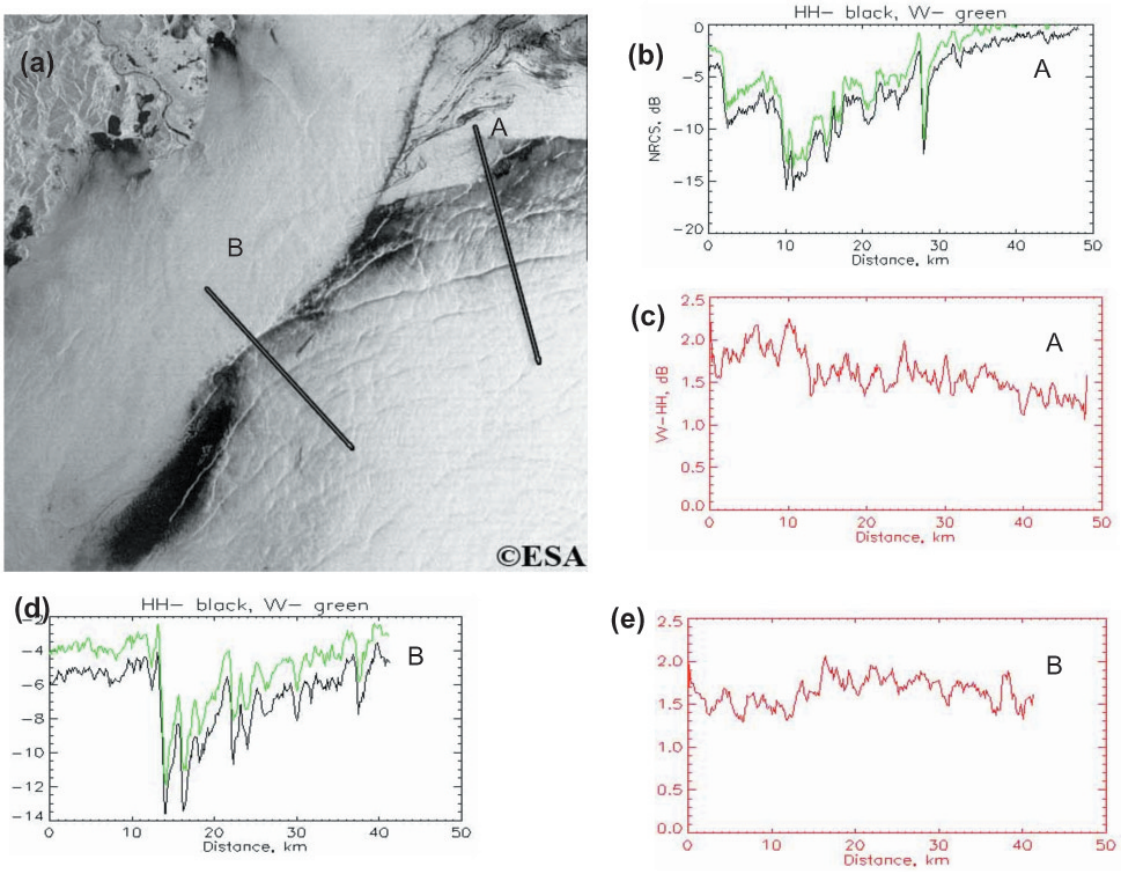

Figure 7. Envisat ASAR image at VV polarization of the south-western part of Peter the Great Bay on 23 September 2004 at 01:36 UTCA showing atmospheric front and a packet of oceanic internal waves propagating onshore (a). Dark lines mark the location of sections A and B. NRCS profiles at VV – (green lines) and HH – (dark lines) polarizations (b) and (d) and polarization ratio profiles (c) and (e) along sections A (b and c) and B (d and e).

of the sea surface roughness were collected during satellite sensing and used to interpret ASAR signatures. The oceanic dynamic phenomena were revealed both on VV- and HH-polarization images in particular when there were slicks on the sea surface. Sea surface wind fields were retrieved with C-band scatterometer function and the variations of a polarization ratio were determined in the areas covered by surface films as well as in the areas where surface imprints of oceanic internal waves were detected. Available data do not allow to conclude whether VV- or HH- polarisation or their combination is generally better for oceanic phenomena study. Probably it was caused by low incidence angle: its average values were 18.3° or 22.5° (Table 1). One cannot, however, rule out the influence of calibration errors, pointing accuracy and polarization isolation on the VV- and HH-polarization data that was mentioned for Envisat APP product in [7]. In connection with this, attention should be given to the analysis of ASAR Alternating Polarisation Mode Complex images (product ID ASA_APS_1P) and to the development of software for processing this product.

ACKNOWLEDGEMENTS

This study has been carried out within project AO3-401 “Mesoscale oceanic and atmospheric phenomena in the coastal area of the Japan and Okhotsk seas: Study with ERS SAR and research vessels”, Envisat project AO-ID-391 “Study of the interaction of oceanic and atmospheric processes in the Japan Sea and the Southern Okhotsk Sea” and an international project BE.2775 “Detection

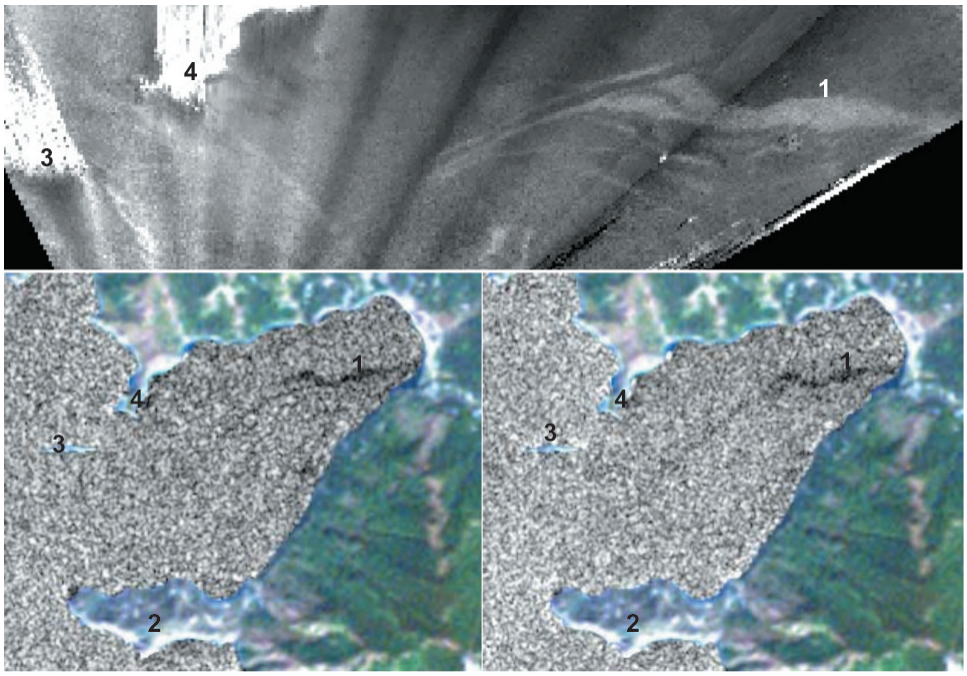

Figure 8. Panoramic image of Vityaz' Bay taken by a coastal video system from Cape Shults and transformed on a plane (a). Light elongated band of variable width is biogenic slick (1). Envisat ASAR image at VV-(b) and HH-(c) polarization of Vityaz' Bay for 20 September 2003. Biogenic slick has a dark tone on both images, however there are differences in its appearance. (2) Cape Shults, (3) – two small islands, (4) – cape on the northern coast of Vityaz' Bay.

and parameter estimation of organic pollution in the coastal zone (DeCOP)." This work is partly supported by Russian State contract for a Project: "Investigation of ocean-atmosphere system with passive and active microwave sensing from new generation satellites" and INTAS Project No. 03-51-4987 "Slicks as Indicators of Marine Processes (SIMP)."

REFERENCES

1. Konstantinov, O.G., 2005. Analysis of the polarizing video images of the sea surface, 2005. In: *Abstract book of 2nd EARSel Workshop on Remote Sensing of the Coastal Zone* (Porto, Portugal), 44.
2. Stoffelen, A.C.M. & Anderson, D.L.T., 1997. Scatterometer data interpretation: Estimation and validation of the transfer function: CMOD4. *J. Geophysical Research*, 102: 5767-5780.
3. Thompson, D.R., Elfouhaily, T.M. & Chapron, B., 1998. Polarization ratio for microwave backscattering from the ocean surface at low to moderate incidence angles, In: *Proc. International Geoscience and Remote Sensing Symposium* (Seattle, WA), 1671-1676.
4. Thompson, D.R. & Beal, R.C., 2000. Mapping high-resolution wind fields using synthetic aperture radar. *The Johns Hopkins Univ. Tech. Dig*., 21: 58-67.
5. Mouchel, A., Hauser, D., Kudryavtsev, V. & Daloze, J.-F., 2005. Multi-polarization ocean radar cross-section from ENVISAT, and airborne polarimetric radar measurements. In: *Envisat & ERS ESA Symposium* (Salzburg, Austria).
6. Mitnik, L.M., Yoon, H-J., Dubina, V.A., Kim, Y-S. & Kim, S.-W., 2003. ERS SAR observations of the Korean coastal waters. In: *The 24th Asian Conference on Remote Sensing & 2003 International Symposium on Remote Sensing* (Busan, Korea), 1: 228-230.
7. Thompson, D.R., Monaldo, F.M., Hortsman, J., Koch, W. & Elfouhaily, T.M., 2005. Impact of Envisat alternating-polarization mode imagery on rough surface scattering models and the generation of high-resolution wind maps. In: *Envisat & ERS ESA Symposium* (Salzburg, Austria).